

## Using Giant Magneto-Impedance Effect for Transportation

Valentina Zhukova, Pablo Rodríguez Jiménez  
Dept. Polymers and Advanced Materials, Univ. Basque  
Country, EHU, 20018 San Sebastian, Spain  
e-mail: valentina.zhukova@ehu.es

Rafael Garcia-Etxabe  
Gaiker Technological Centre, 48170, Zamudio, Spain  
e-mail: etxabe@gaiker.es

Mohamed Salaheldeen  
Dept. Polymers and Advanced Materials, Univ. Basque  
Country, EHU, 20018 San Sebastian, Spain and Phys. Dept.,  
Faculty of Science, Sohag University, Sohag 82524, Egypt  
e-mail: mohamed.salaheldeenmohamed@ehu.eus

Arcady Zhukov  
Dept. Applied Physics, Univ. Basque Country, EIG, EHU,  
20018, San Sebastian, and Ikerbasque, Basque Foundation  
for Science, Spain  
e-mail: arkadi.joukov@ehu.es

**Abstract**— Ferromagnetic amorphous microwires exhibit magnetic properties, as well as Giant magneto-Impedance (GMI) which are sensitive to external stimuli, such as stress or heating, making them suitable for the development of various sensors. On the other hand, the use of Taylor-Ulitovsky fabrication technique allows to produce such microwires covered with insulating flexible glass coating and with the widest range of diameters (from 0.1 to 100  $\mu\text{m}$ ). We provide experimental results on dependencies of the hysteresis loops and GMI effect of glass-coated microwires on external stimuli. The obtained results are considered as a base for a novel sensing technique allowing non-destructive and non-contact monitoring utilizing ferromagnetic glass-coated microwire for various applications, such as transportation (aircraft, automobile and railroad sectors).

**Keywords** - giant magnetoimpedance effect; magnetic microwires; magnetic softness; smart composites.

### I. INTRODUCTION

Amorphous magnetic materials, discovered in 60-s, commonly present an unusual combination of excellent magnetic properties (e.g., high magnetic permeability, giant magnetoimpedance, GMI, effect, magnetic bistability, Matteucci and Widemann effects) together with superior mechanical properties (plasticity, flexibility) [1]-[5]. Such combination of physical properties makes them attractive for various technological applications [6]-[8]. Enhanced magnetic softness of amorphous materials is linked to the disordered structure characterized by the absence of the magnetocrystalline anisotropy and defects (dislocations, grain boundaries, etc.) typical for conventional crystalline magnets [1]-[5]. The manufacturing techniques of different types of amorphous materials involves rapid melt quenching [1]-[4]. Such fabrication techniques are generally quite fast and not expensive, allowing preparation of soft magnetic materials without any complex post-processing treatments [1]-[4].

For many applications, especially in the transport (automotive or aviation industries) or medicine, new features such as reduced size, increased corrosion resistance or

biocompatibility are in high demand. Therefore, much attention is paid to the development of alternative manufacturing methods that allow obtaining amorphous materials with insulating coatings at the micro- and nanoscale using rapid quenching of the melt [6]-[8].

Glass-coated microwires fabricated by the Taylor-Ulitovsky method meet most of the above-mentioned requirements: such magnetic microwires have micro-nanometer diameters (typically 0.1-100  $\mu\text{m}$ ), they are covered with a thin, insulating, biocompatible and flexible glass coating [7]-[11], and can have excellent magnetic softness, high GMI effect or magnetic bistability [9]-[11].

This combination of properties of glass-coated amorphous microwires allows for development of new technological applications, such as magnetic sensors [6]-[9] [12]-[14] or smart composites with tunable magnetic permittivity [8][15].

Recently, the stress and temperature dependence of hysteresis loops and GMI effect are proposed for the development of smart composites with microwires inclusions and magnetoelastic sensors or using magnetoelastic sensors based on stress dependence of various magnetic properties [12]-[19].

In this work, we provide our results on study of the influence of stresses and temperature on GMI effect and magnetic properties of glass-coated microwires paying attention on applications in transportation industries, such as aircraft, automobile or railroad sectors.

The rest of the paper is structured as follows. In Section II, we present the experimental methods, while in Section III we describe the results on the stress and temperature dependencies of the hysteresis loops and the GMI effect of the studied microwires. The article concludes in Section IV.

### II. EXPERIMENTAL DETAILS

We studied Co and Fe-rich glass-coated amorphous microwires with metallic nucleus diameters,  $d$ , between 15 and 40  $\mu\text{m}$  prepared by the aforementioned Taylor-Ulitovsky method. Briefly, the fabrication method consists

of melting a metallic alloy ingot inside a glass (typically Duran or Pyrex) tube using a high-frequency inductor, forming the glass capillary from softened glass, drawing of such capillary filled with the molten metallic alloy and winding of the solidified glass-coated microwires onto a rotating bobbin [9][10].

The hysteresis loops were measured by the fluxmetric method using a specially designed setup for studying soft magnetic microwires of reduced diameter [20]. To avoid the error associated with precise evaluation of the magnetic nucleus diameter we represented the hysteresis loops as the normalized magnetization  $M/M_o$  (where  $M_o$  is the magnetic moment of the samples at maximum magnetic field amplitude,  $H_o$ ) versus  $H$ .

The GMI ratio,  $\Delta Z/Z$ , was defined using the commonly  $\Delta Z/Z$  definition, as [3][4][7]:

$$\Delta Z/Z = [Z(H) - Z(H_{max})] / Z(H_{max}) \cdot 100 \quad (1)$$

where  $Z$  is wire impedance,  $H_{max}$  – is the maximum applied DC magnetic field (typically below a few kA/m).

Wire impedance,  $Z$ , was experimentally measured reflection coefficient  $S_{11}$  using a vector network analyzer using the expression:

$$Z = Z_o \frac{(1+S_{11})}{(1-S_{11})} \quad (2)$$

where  $Z_o = 50$  Ohm is the characteristic impedance of the coaxial line. Use of the specially designed sample holder with coaxial line connections allows to measure  $Z(H)$  dependencies up to GHz frequencies [21].

For wireless measurements of microwire response under stress at 2.45 GHz, we used the free space measurement system, consisting of two broadband horn antennas fixed to the anechoic chamber and a vector network analyzer, previously used for the composites characterization at free space [15]. We measured the scattering  $S_{22}$ , parameter. As recently proposed [18], the AC modulating magnetic field was applied parallel to the ferromagnetic microwires to modulate the impedance in the microwire. We use the same modulation magnetic field frequency,  $f$ , of 80 Hz as in our previous studies [18].

The applied stresses value,  $\sigma$ , acting on the metallic nucleus has been evaluated considering different Young's moduli of the metallic alloy and the glass,  $E_1$  and  $E_2$  respectively, as was described earlier [22]:

$$\sigma = \frac{K \cdot P}{K \cdot S_m + S_{gl}} \quad (3)$$

where  $k = E_2/E_1$ ,  $P$  - the applied mechanical load, and  $S_m$  and  $S_{gl}$  are the cross sections of the metallic nucleus and glass coating respectively.

### III. EXPERIMENTAL RESULTS AND DISCUSSION

As expected from previous studies [9], as-prepared Fe-rich and Co-rich microwires present rather different

hysteresis loops. As shown in Figure 1, Fe-rich ( $\text{Fe}_{75}\text{B}_9\text{Si}_{12}\text{C}_4$ ) microwires present rectangular hysteresis loops. While, Co-rich ( $\text{Co}_{65.4}\text{Fe}_{3.8}\text{Ni}_{13.8}\text{B}_{13.8}\text{Si}_{13}\text{Mo}_{1.35}\text{C}_{1.65}$ ) microwires present different kind of hysteresis loop with low coercivity and high initial permeability. From the hysteresis loops, we can evaluate the coercivity,  $H_c$ , and the switching field,  $H_s$  (for the case of rectangular hysteresis loops, see Figure 1a) and magnetic anisotropy field,  $H_k$  (for the case of linear hysteresis loops, Figure 1b). It is worth mentioning that  $H_c$ ,  $H_s$  and  $H_k$  – values are significantly affected by magnetic field frequency,  $f$ , and amplitude,  $H_o$  [23]. Therefore, all the measurements have been performed at fixed  $f$  (100 Hz) and  $H_o$  values.

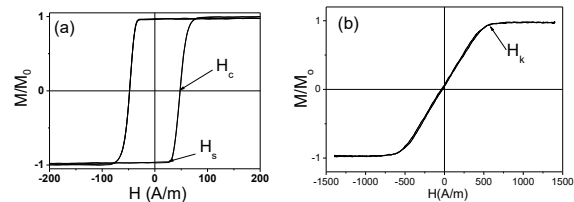


Figure 1. Typical rectangular ( $\text{Fe}_{75}\text{B}_9\text{Si}_{12}\text{C}_4$  microwire) (a) and linear ( $\text{Co}_{65.4}\text{Fe}_{3.8}\text{Ni}_{13.8}\text{B}_{13.8}\text{Si}_{13}\text{Mo}_{1.35}\text{C}_{1.65}$  microwire) (b) hysteresis loops of magnetic microwires illustrating definitions of  $H_c$ ,  $H_s$  and  $H_k$ .

We observed that the shape of the hysteresis loops of Co-rich ( $\text{Co}_{65.4}\text{Fe}_{3.8}\text{Ni}_{13.8}\text{B}_{13.8}\text{Si}_{13}\text{Mo}_{1.35}\text{C}_{1.65}$ ) microwires remains almost the same (linear with low coercivity) when stress is applied. However, an increase in the magnetic anisotropy field,  $H_k$ , can be observed upon tensile stress,  $\sigma$  (see Figure 2b). The origin of such linear  $H_k(\sigma)$  dependence was recently discussed in terms of the stress dependence of the magnetoelastic anisotropy,  $K_{me}$ , given as [24]:

$$K_{me} = 3/2 \lambda_s \sigma \quad (4)$$

where  $\lambda_s$  is the magnetostriction coefficient.

As shown in Figure 3a, when the tensile stress is applied the character of hysteresis loops of Fe-rich ( $\text{Fe}_{75}\text{B}_9\text{Si}_{12}\text{C}_4$ ) microwires does not change, although an increase in  $H_c$  is observed. Evaluated  $H_c(\sigma)$  and  $H_s(\sigma)$  are shown in Figure 3b. As can be appreciated, both  $H_c$  and  $H_s$  present similar tendency showing increase upon applied stress.

Previously,  $H_s(\sigma)$  dependence was interpreted considering that the  $H_s$  is proportional to the energy required to form the domain wall,  $\gamma$ , involved in the bistable magnetization process. The domain wall energy linked with  $K_{me}$  and hence with  $\sigma$  and then it can be expressed as [25]:

$$H_s \propto \gamma \propto \frac{[A(3/2) \lambda_s (\sigma + \sigma_r)]^{1/2}}{\cos \alpha} \quad (5)$$

where  $\alpha$  is the angle between magnetization and axial direction,  $A$  is the exchange energy constant, and  $\sigma_r$  is the residual tensile stress. Consequently,  $H_s$  must be proportional to  $\sigma^{1/2}$  for  $\sigma$  larger than  $\sigma_r$  and  $\cos \alpha \approx 1$ .

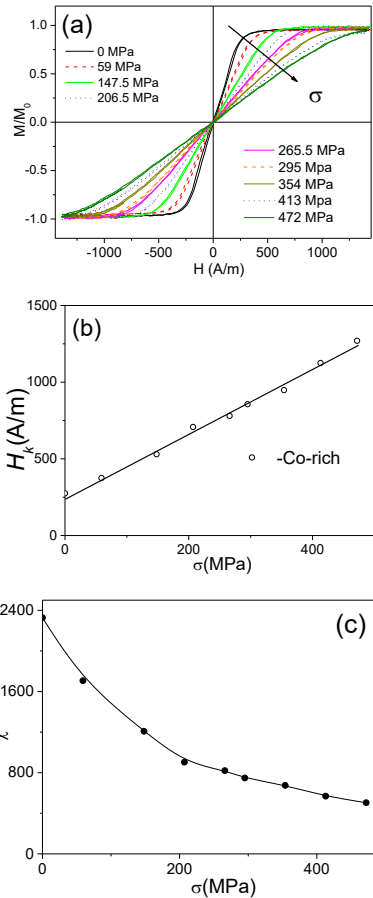


Figure 2. Effect of applied stress on hysteresis loops (a)  $H_k(\sigma)$  dependence (b) and  $\chi(\sigma)$  (c) of  $Co_{65.4}Fe_{3.8}Ni_1B_{13.8}Si_{13}Mo_{1.35}C_{1.65}$  microwires.

The experimentally observed  $H_s(\sigma)$  and  $H_c(\sigma)$  dependencies better fits to  $H_c \sim \sigma^{0.74}$  and  $H_s \sim \sigma^{0.58}$  (see Figure 3b). Qualitatively, a fairly good agreement is observed between the predicted and experimental  $H_s(\sigma)$  and  $H_c(\sigma)$  dependencies.

The observed difference in predicted and experimentally observed  $H_c(\sigma)$  and  $H_s(\sigma)$  dependencies must be attributed to complex internal stresses [26]. Additionally, although the origin of the switching field,  $H_s$ , is linked with the domain wall nucleation or depinning processes, the coercivity,  $H_c$ , is also affected by the velocity of the propagating domain wall [23].

Influence of temperature on hysteresis loops of Fe-rich and Co-rich microwire is shown in Figure 4. It is remarkable that upon heating the hysteresis loops of Fe-rich microwires become essentially non-rectangular. Rectangular hysteresis loop transforms into inclined upon heating (with an increase in T). The opposite tendency is observed for Co-rich microwires: upon heating the hysteresis loops becomes almost rectangular (see Figure 4b).

Accordingly, the GMI effect is also affected substantially by temperature (see Figure 5). An increase in  $\Delta Z/Z$ -value is observed for Fe-rich microwire being most

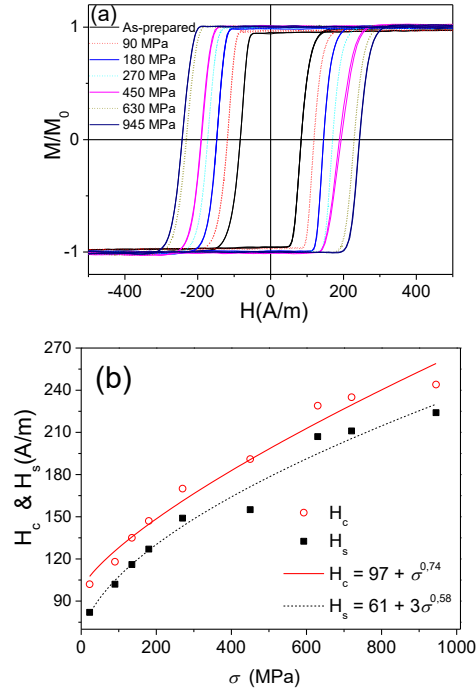


Figure 3. Effect of applied stresses on hysteresis loops (a) and  $H_c(\sigma)$  and  $H_s(\sigma)$  dependencies (b) of  $Fe_{75}B_9Si_{12}C_4$  microwires. The experimental  $H_s(\sigma)$  and  $H_c(\sigma)$  dependencies are compared with fitting considering  $H_c(\sigma=0)=97$  A/m and  $H_s(\sigma=0)=61$  A/m.

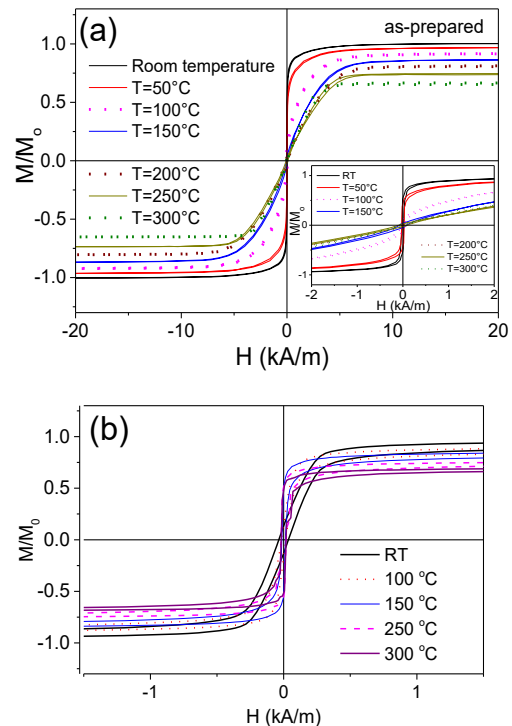


Figure 4. Hysteresis loops of Fe-rich (a) and Co-rich (b) microwire measured at different T.

remarkable at  $T=300$  °C: Maximum GMI ratio,  $\Delta Z/Z_{max} \approx 120\%$  is recorded at  $T=300$  °C (100 MHz) (Figure 5a). While

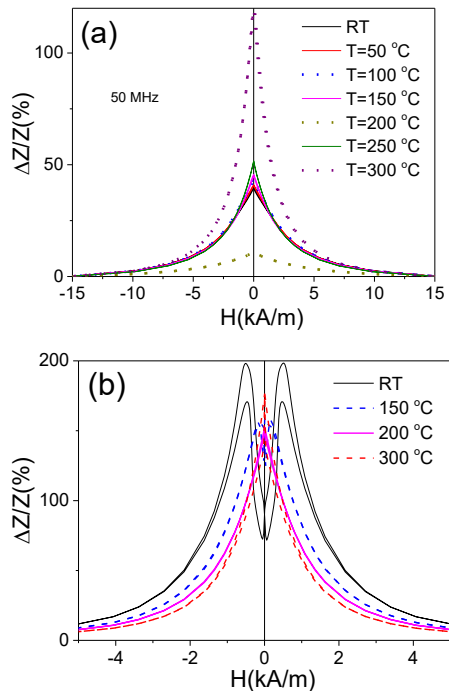


Figure 5.  $\Delta Z/Z(H)$  dependencies of Fe-rich (a) and Co-rich (b) microwires measured at 50 MHz at various temperatures.

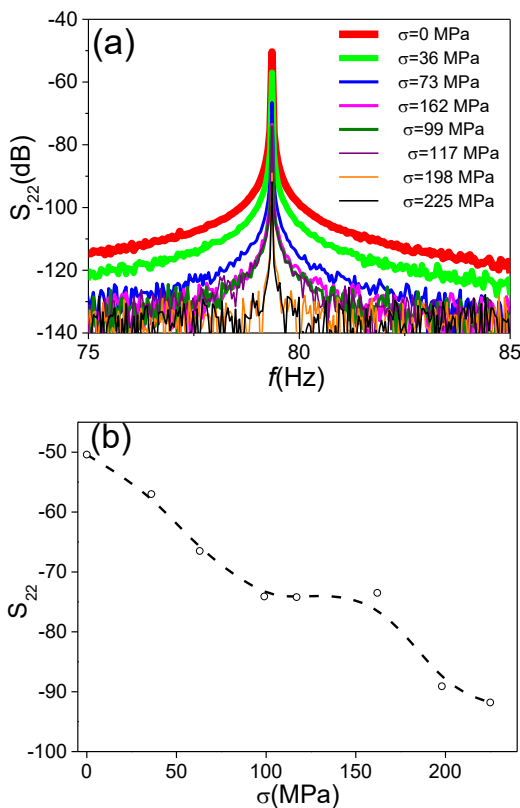


Figure 6. Frequency Spectrum of  $S_{22}$  module (a) and effect of applied stress on amplitude of the 1<sup>st</sup> harmonic (fundamental, 80 Hz) of  $S_{22}$  at different  $\sigma$ -values (b).

in Co-rich microwire the opposite tendency (a decrease in  $\Delta Z/Z_{max}$  upon heating) is observed (see Figure 5b).

As described above, we measured the influence of applied stress,  $\sigma$ , on microwave signal of single microwire. A low frequency AC magnetic field (80 Hz) was applied by a planar coil placed inside the anechoic chamber. Using the VNA we measured the  $S_{22}$  parameters at 2.45 GHz at different  $\sigma$ -values. The  $S_{22}(\sigma)$  dependence is provided in Figure 6a. A substantial decay of the  $S_{22}$  parameter measured at 2.45 GHz is observed (see Figure 6a). The dependence of  $S_{22}$  on  $\sigma$ , evaluated from Figure 6a, is provided in Figure 6b. From Figure 6b is evident that upon the applied stress from 0 to 225 MPa,  $S_{22}$  changes on 40 dB (100 times) from -50 to -90 dB.

The observed substantial  $S_{22}(\sigma)$  dependence can be explained considering the  $\chi(\sigma)$  dependence provided in Figure 2c.

The observed dependencies of magnetic properties, GMI effect and even  $S_{22}$  at microwave frequencies are potentially suitable for exciting applications in structural integrity and health monitoring related to wireless stresses monitoring and integrity in civil engineering, aircraft and automobile industries.

Certainly, contactless stress monitoring in carbon fiber composite materials for the aircraft industry is vital to the safety of modern aircrafts. In these applications glass-coated microwires inclusions with high GMI effect embedded in composites with enhanced corrosion resistance and mechanical properties are responsible for remote stresses or temperature monitoring in aircraft and car industries [18][27].

The peculiarity of the composites used for aircraft industry is the presence of the carbon fibers making such composites conductive. Therefore, further developments were needed to separate the microwave response of magnetic microwires from that of conductive carbon fibres. Recently, this problem has been successfully solved using a low frequency modulated magnetic field [18]. For such applications, high GMI effect and high stress sensitivity of the microwave response of magnetic microwires are essentially relevant.

The main advantage of the microwave stress and temperature monitoring (using  $S$ - parameters) is the possibility of contactless measurements at large distance to the microwire [8][27][28]. Additionally, the changes in  $S_{22}$ - parameter are rather large (see Figure 6). In contrast, changes in  $H_c$  and  $H_s$  are smaller (see Figure 3). Additionally, the distance to such magnetically bistable microwire is usually limited to a few cm [29]. However, the low frequency measurements (such as dependence of coercivity on external stimuli) are less affected by the matrix conductivity.

#### IV. CONCLUSIONS AND FUTURE WORK

We demonstrated that magnetic properties, GMI effect and microwave signal produced by ferromagnetic

microwires are substantially affected by mechanical stress and heating.

The obtained experimental results yield new and important insights suitable for development of sensing technique for non-destructive and non-contact monitoring of the composites containing embedded microwire inclusions for aircraft, automobile industries.

#### ACKNOWLEDGMENT

This work was supported by Spanish MCIU under PGC2018-099530-B-C31 (MCIU/AEI/FEDER, UE) by EU under “Harmony” (HORIZON-CL4-2023-RESILIENCE-01) project and by the Government of the Basque Country under Elkartek (ATLANTIS and MOSINCO) projects. The authors are thankful for the technical and human support provided by SGIker of UPV/EHU (Medidas Magnéticas Gipuzkoa) and European funding (ERDF and ESF).

#### REFERENCES

- [1] J. Durand, “Magnetic Properties of Metallic Glasses” in Topics in Applied Physics Volume 53, 1983, Glassy Metals II. Atomic Structure and Dynamics, Electronic Structure, Magnetic Properties, Editors: H. Beck and H.-J. Güntherodt, Springer-Verlag, Berlin Heidelberg New York Tokyo.
- [2] G. Herzer, Amorphous and Nanocrystalline Materials, in: Encyclopedia of Materials: Science and Technology, pp. 149–157, Elsevier Science Ltd., 2001, ISBN: 0-08-0431526.
- [3] A. P. Zhukov, “The remagnetization process of bistable amorphous alloys”, Mater. Design, vol. 5, pp. 299-305, 1993.
- [4] M. Hagiwara, A. Inoue, and T. Masumoto, “Mechanical properties of Fe-Si-B amorphous wires produced by in-rotating-water spinning method”, Metall. Trans. A vol. 13, pp. 373-382, 1982.
- [5] T. Goto, M. Nagano, and N. Wehara, “Mechanical properties of amorphous Fe<sub>80</sub>P<sub>16</sub>C<sub>3</sub>B<sub>1</sub> filament produced by glass-coated melt spinning”, Trans. JIM, vol. 18, pp. 759-764, 1997.
- [6] D. Kozejova et al., “Biomedical applications of glass-coated microwires”, J. Magn. Mater., vol. 470, pp. 2-5, 2019.
- [7] A. F. Cobeño et al., “Magnetoelastic sensor based on GMI of amorphous microwire”, Sens. Actuators A, vol. 91, pp. 95-98, 2001.
- [8] L. Panina, M. Ipatov, V. Zhukova, J. Gonzalez, and A. Zhukov, “Tuneable composites containing magnetic microwires”, ch. 22, pp.431-460 DOI: 10.5772/21423 in Book: Metal, ceramic and polymeric composites for various uses, Edited by John Cuppoletti, 2011, DOI: 10.5772/1428 ISBN: 978-953-307-353-8 (ISBN 978-953-307-1098-3) InTech - Open Access Publisher (www.intechweb.org), Janeza Trdine, 9, 51000 Rijeka, Croatia.
- [9] V. Zhukova et al., “Development of Magnetically Soft Amorphous Microwires for Technological Applications”, Chemosensors, vol. 10, p. 26, 2022.
- [10] H. Chiriac, S. Corodeanu, M. Lostun, G. Ababei, and T.-A. Óvári, “Rapidly solidified amorphous nanowires”, J. Appl. Phys., vol. 107, 09A301, 2010.
- [11] P. Corte-Leon et al., “The effect of annealing on magnetic properties of “Thick” microwires”, J. Alloys Compounds vol. 831, p.150992,2020, doi: https://doi.org/10.1016/j.jallcom.2019.06.094
- [12] A. Zhukov et al., “Magnetoelastic sensor of level of the liquid based on magnetoelastic properties of Co-rich microwires”, Sens. Actuat. A Phys., vol 81, no. 1-3, pp.129-133, 2000.
- [13] A. Talaat et al., “Ferromagnetic glass-coated microwires with good heating properties for magnetic hyperthermia”, Sci. Reports, vol. 6, p. 39300, 2016.
- [14] M. Churyukanova et al., “Non-contact method for stress monitoring based on stress dependence of magnetic properties of Fe-based microwires”, J. Alloys Compd., vol. 748(5) pp. 199-205, 2018.
- [15] D. Makhnovskiy, A. Zhukov, V. Zhukova, and J. Gonzalez, “Tunable and self-sensing microwave composite materials incorporating ferromagnetic microwires”, Advances in Science and Technology, vol. 54, pp. 201-210, 2008.
- [16] D. Praslička et al., “Possibilities of Measuring Stress and Health Monitoring in Materials Using Contact-Less Sensor Based on Magnetic Microwires”, IEEE Trans. Magn., vol. 49(1), pp. 128-131, 2013.
- [17] A. Allue et al., “Smart composites with embedded magnetic microwire inclusions allowing non-contact stresses and temperature monitoring”, Compos. Part A Appl., vol. 120, pp. 12-20, 2019, DOI: 10.1016/j.compositesa.2019.02.014.
- [18] V. Zhukova et al., “Free Space Microwave Sensing of Carbon Fiber Composites with Ferromagnetic Microwire Inclusions”, IEEE Sens. Lett., vol. 8, No. 1, p. 2500104, 2024.
- [19] P. Corte -Leon et al., “Effect of temperature on magnetic properties and magnetoimpedance effect in Fe -rich microwires”, J. Alloys Compound. vol. 946, p.169419, 2023, doi: https://doi.org/10.1016/j.jallcom.2023.169419
- [20] L. Gonzalez-Legarreta et al., “Optimization of magnetic properties and GMI effect of Thin Co-rich Microwires for GMI Microsensors,” Sensors, vol. 20, p.1558, 2020.
- [21] A. Zhukov et al., “Routes for Optimization of Giant Magnetoimpedance Effect in Magnetic Microwires”, IEEE Instrumentation & Measurement Magazine, vol. 23, no. 1, pp. 56-63, 2020, doi: 10.1109/MIM.2020.8979525.
- [22] V. Zhukova, M. Ipatov, and A. Zhukov, “Microwave stress monitoring using Co-rich amorphous microwire assessed by free space measurements”, J. Sci.: Adv. Mater. Devices, vol.10, p.100950, 2025 doi: https://doi.org/10.1016/j.jsamd.2025.100950.
- [23] A. Zhukov et al., “Frequency dependence of coercivity in rapidly quenched amorphous materials”, J. Mat. Sci. Eng. A vol. 226-228, pp. 753-756, 1997.
- [24] P. Corte-Leon et al., “Stress dependence of the magnetic properties of glass-coated amorphous microwires” J. Alloys Compound, vol. 789, pp. 201-208, 2019, doi: 10.1016/j.jallcom.2019.03.044
- [25] P. Aragonese et al., “The Stress dependence of the switching field in glass-coated amorphous microwires”, J. Phys. D: Applied Phys. vol. 31, pp. 3040-3045, 1998.
- [26] A. Zhukov et al., “Ferromagnetic resonance and Structure of Fe-based Glass-coated Microwires,” J. Magn. Magn. Mater., vol. 203, pp. 238-240, 1999.
- [27] M. Ipatov et al., “Tunable effective permittivity of composites based on ferromagnetic microwires with high magneto-impedance effect”, Appl. Phys. A, vol. 103(3), pp. 693-697, 2011.
- [28] R. Garcia-Etxabe et al., “Influence of Tensile Stress on Microwave Scattering Parameters of Continuous Ferromagnetic Microwire Embedded into Glass Reinforced Composites”, IEEE Trans. Magn., vol. 61(6), p. 4001004, 2025.
- [29] S. Gudoshnikov et al., “Evaluation of use of magnetically bistable microwires for magnetic labels”, Phys. Status Solidi A, 208, No. 3, 526–529 (2011)/ DOI 10.1002/pssa.201026414.